Supporting Information
Edge-driven adatom kinetics in graphene nanoribbons growth on Cu(111)

Alexandr Alexeev, Sergey N. Filimonov

Department of Physics, National Research Tomsk State University, 36 Lenin Ave., 634050 Tomsk, Russia
*Email: a.a.o@mail.tsu.ru

1 Adatom energies and diffusion barriers

Here we report calculated energies and diffusion barriers of carbon adatoms in the vicinity of the edge of a graphene nanoribbon (GNR) supported on Cu(111). The adatom energy is defined as:

$$E_{ad} = E_{sub+C} - E_{sub} - E_C, \tag{1}$$

where E_{sub+C} is the total energy of the substrate with a carbon adatom, E_{sub} is the total energy of the substrate without the adatom, and E_C is the energy of an isolated carbon atom.

Tables S1, S2 and S3 present the calculated adsorption energies and surface diffusion barriers for carbon adatoms at various sites on the Cu(111) surface and on the zigzag (ZGNR) and armchair (AGNR) graphene nanoribbons. The adsorption sites are denoted as follows. Letters indicate the high-symmetry adsorption positions:

- F: fcc hollow site on Cu(111);
- H: hcp hollow site on Cu(111);
- T: top site (atop a copper atom) on Cu(111);
- B: bridge site on the graphene layer.

Numbers indicate the relative distance from the graphene edge, with a lower number corresponding to a position closer to the edge. For instance, F1 denotes the fcc site on copper nearest to the step edge, while F3 represents a site located further away. The width of the GNR is measured in the number of benzene rings (2-ring, 3-ring, etc.)

Table S1: Energies of carbon adatoms near the ZGNR edge.

site	E_{ad}, eV			
	2 rings	3 rings	4 rings	5 rings
B6				-3.16
B5			-3.45	-3.25
B4		-4.27	-3.67	-3.39
B3	-4.55	-3.94	-3.71	-3.65
B2	-5.38	-4.80	-4.53	-4.48
edge	-7.17	-6.88	-6.79	-6.71
H2	-5.92	-5.98	-6.04	-6.03
F3	-6.25	-6.28	-6.28	-6.26
H4	-6.22	-6.24	-6.20	-6.21
F5	-6.33	-6.36	-6.32	-6.33
H6	-6.26	-6.28	-6.26	-6.27
F7	-6.32	-6.32	-6.30	-6.32
F1	-6.64	-6.02	-5.98	-5.85

Table S2: Diffusion barriers for carbon adatoms near the ZGNR edge.

sites	E_{dif}, eV			
	2 rings		5 rings	
	$\leftarrow$	$\rightarrow$	$\leftarrow$	$\rightarrow$
B6 $\leftrightarrow$ B5			0.63	0.54
B5 $\leftrightarrow$ B4			0.83	0.69
B4 $\leftrightarrow$ B3			0.92	0.66
B3 $\leftrightarrow$ B2			1.44	0.62
B2 $\leftrightarrow$ edge	2.68	0.89	2.93	0.70
edge $\leftrightarrow$ H2	0.05	1.30	0.22	0.90
H2 $\leftrightarrow$ F3	0.39	0.06	0.31	0.08
F3 $\leftrightarrow$ H4			0.22	0.27
F1 $\leftrightarrow$ H2			0.44	0.27

Table S3: Energies of carbon adatoms near the AGNR edge.

site	E_{ad}, eV		
	3 rings	4 rings	5 rings
B5			-3.18
B4		-3.47	-3.27
B3	-4.00	-3.67	-3.56
B2	-4.44	-4.28	-4.25
H0	-7.83	-7.92	-8.03
F0	-7.82	-7.93	-8.03
T0	-8.29	-8.30	-8.37
T1	-7.28	-7.20	-7.22
H2	-6.10	-6.15	-6.19
F2	-6.17	-6.22	-6.27
H3	-6.33	-6.31	-6.33
F3	-6.39	-6.38	-6.40
H4	-6.33	-6.32	-6.36
F4	-6.39	-6.38	-6.42
H5	-6.30	-6.28	-6.31
F5	-6.36	-6.34	-6.37
H6	-6.32	-6.32	-6.33
F6	-6.39	-6.38	-6.39

2 Structure of armchair graphene nanoribbon on Cu(111)

Figure S1 shows the optimized geometry of a five-ring armchair graphene nanoribbon on Cu(111) after attachment of a carbon adatom to the graphene edge at the energetically favorable T0 site. Following adatom attachment, a significant local reconstruction of the ribbon edge is observed in the immediate vicinity of the adsorption site.

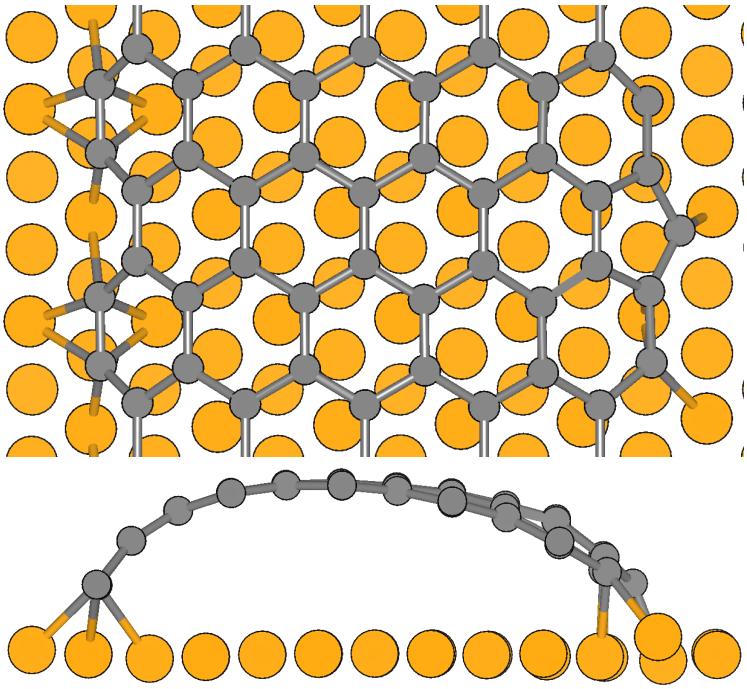

Figure S1: Top and side views of a five-ring AGNR on Cu(111) with the attached carbon adatom.

3 Adatom energy and nanoribbon curvature

Figure S2 shows adatom energy at different adsorption positions as a function of the GNR width. In can be seen that the strength of adatom bonding systematically varies with GNR width, being most pronounced for the narrowest ribbons. At the central region of a five-ring ZGNR the adatom energy reaches the value expected for an infinite graphene sheet on Cu(111). That is the most dramatic finite-size effects occur at the GNR widths below 4–5 rings, and adatom properties are expected to converge asymptotically for wider ribbons.

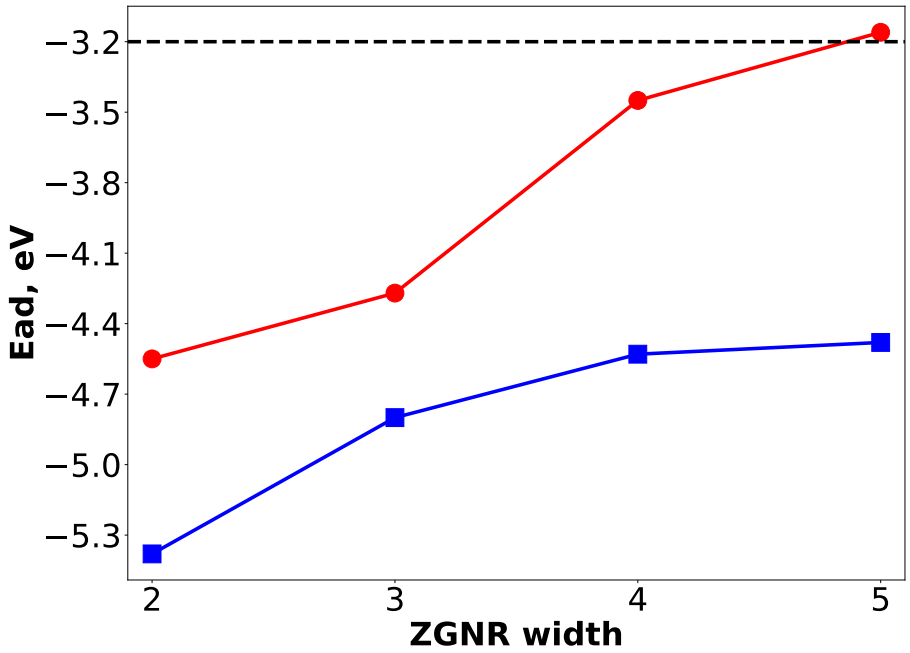

Figure S2: Adatom energy at the ZGNR center (red) and at the B2 site near the ZGNR edge (blue) as a function of the GNR width. The dashed line shows the adatom energy on the infinite graphene sheet on Cu(111).

Fig. S3 shows the average GNR curvature (excluding the edge atoms) as a function of GNR width. The arc-shape of the GNR is a direct consequence of the edge-substrate bonding. With the increasing GNR width the central GNR region flattens. This flattening is manifested by the decreasing GNR curvature and correlates with the decreasing adatom energies. Therefore, the convergence of the geometric shape (flattening) and the convergence of the adsorption energies are directly linked processes.

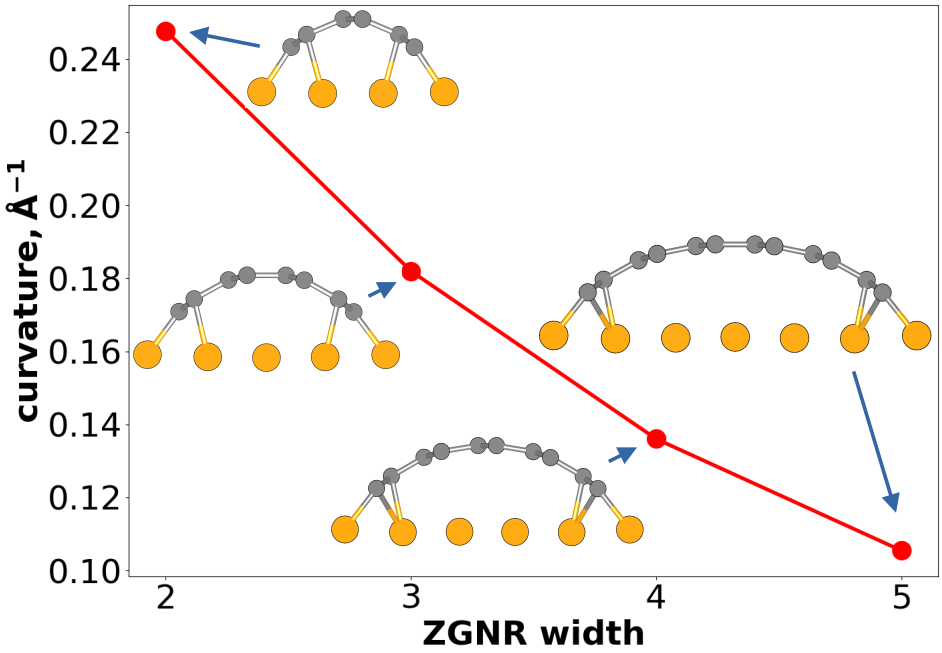

Figure S3: Curvature of zigzag graphene nanoribbons of various widths.

4 Lattice deformations

The lattice deformations are characterized by the strain tensor ε_{ij} given by:

$$\varepsilon_{ij} = \frac{1}{2}\left(\frac{\partial u_i}{\partial x_j} + \frac{\partial u_j}{\partial x_i}\right), \tag{2}$$

where $u_i = x'_i - x_i$ are components of the lattice displacement vector, x'_i and x_i are the coordinates of an atom in the deformed and non-deformed lattice, respectively. The distributions of the lateral component of the strain tensor ε_{xx} near the edge of ZGNRs of various width are shown in Fig. S4.

As can be seen, the copper surface is compressed near the GNR edge. The strain decreases with increasing ZGNR width.

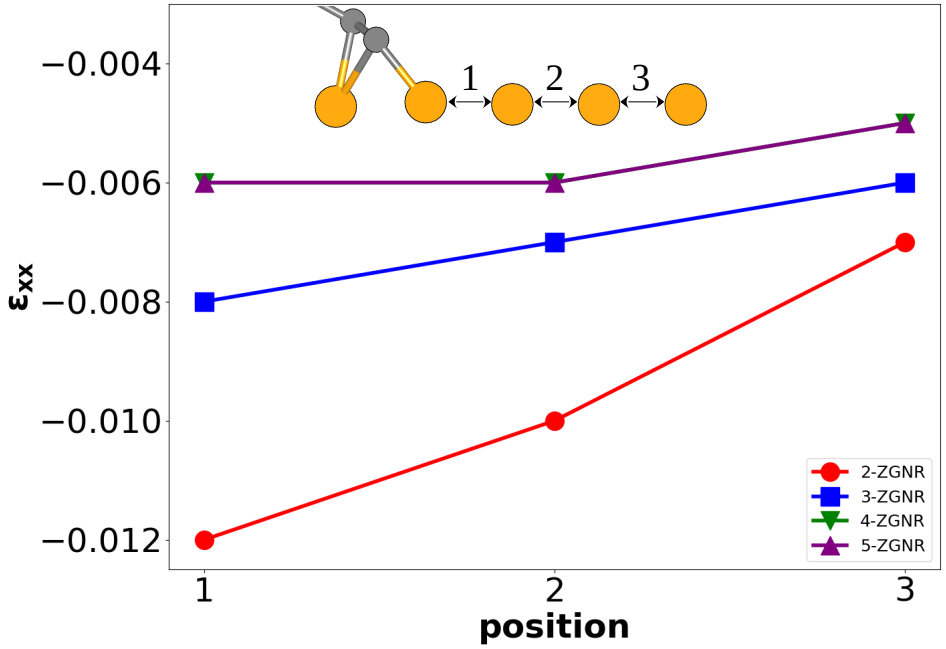

Figure S4: Lateral component of the strain tensor ε_{xx} of the substrate near the ZGNR edge.

5 Role of the adatom drift

To quantitatively assess how the predicted drift of carbon adatoms toward the graphene edges affects the GNR growth kinetics, we performed kinetic Monte Carlo (kMC) simulations. The model considers a one-dimensional representation of the GNR surface and includes the following key processes (Fig. S5):

1. Surface diffusion of carbon adatoms on the GNR with an activation barrier of 0.55 eV, modified by an energy bias. This bias is implemented as a position-dependent correction to the diffusion barrier, derived from the DFT-calculated energy gradient.

2. Attachment to the GNR edge via the identified low-barrier push-out mechanism, with a barrier of 0.7 eV.

3. A competing process of adatom intercalation to the graphene-metal interface with a calculated barrier of 0.77 eV.

In each simulation run, an adatom starts at a random position on the GNR and undergoes a random walk until it either attaches to the edge or intercalates beneath the graphene layer. The attachment probability is computed as the fraction of simulation runs ending with adatom attachment.

The simulation results in Fig. S6 reveal that at a temperature range of 300–800 K substantial fraction of carbon adatoms intercalates to the GNR/Cu(111) interface. On a longer time scale this would contribute to the second layer nucleation beneath the growing GNR. The attachment probability is enhanced by 20–30% when the energy bias is included. Thus we conclude that the adatom drift is a kinetically decisive factor that helps to maintain a single-layer growth mode of graphene by steering adatoms to the GNR edges before they intercalate.

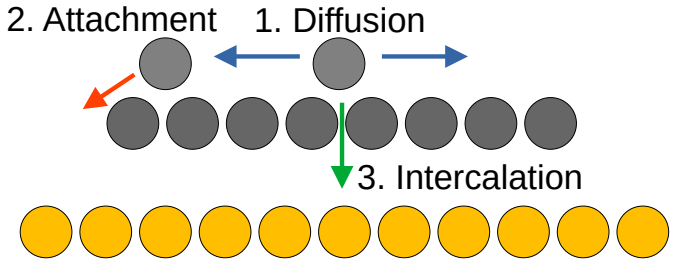

Figure S5: Elementary kinetic processes implemented in the kMC model.

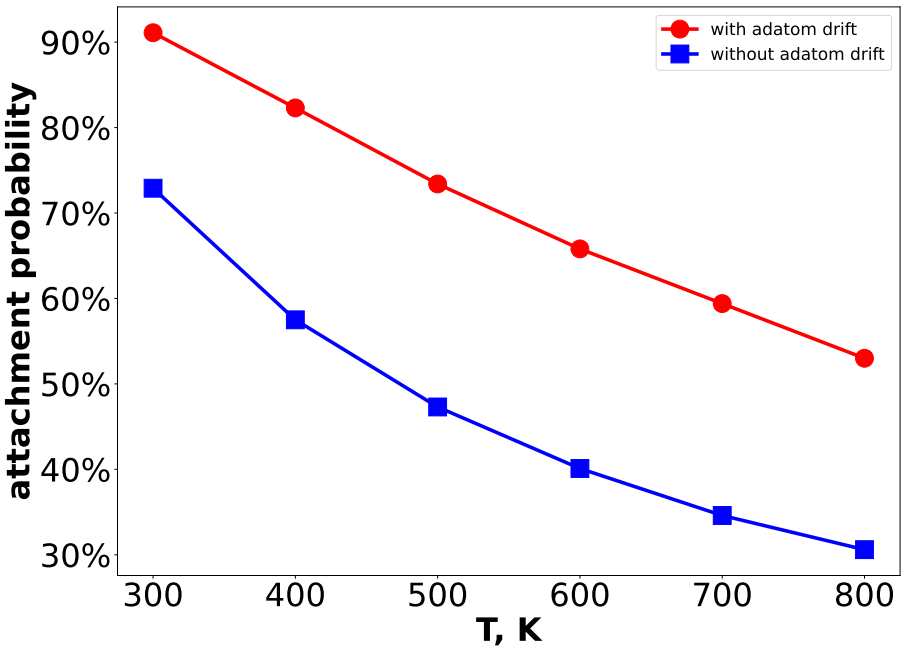

Figure S6: Temperature dependence of the attachment probability of carbon adatoms.